Engineering Geology 127 (2012) 65–74

Contents lists available at SciVerse ScienceDirect

Engineering Geology

journal homepage: www.elsevier.com/locate/enggeo

An analysis of reservoir conditions and responses in longwall panel overburden during mining and its effect on gob gas well performance

Steven J. Schatzel *, C. Özgen Karacan, Heather Dougherty, Gerrit V.R. Goodman

National Institute for Occupational Safety and Health, Office of Mine Safety and Health Research, PO Box 18070, Pittsburgh, PA, 15236, United States

ARTICLE INFO

Article history:
Received 3 December 2010
Received in revised form 31 December 2011
Accepted 5 January 2012
Available online 12 January 2012

Keywords:
Underground mining
Ventilation
Explosions
Subsidence

ABSTRACT

NIOSH conducted a cooperative research study to provide direct measurements of changing reservoir conditions in longwall panel overburden. The field measurements documented changes in permeabilities, methane concentrations, fluid pressures, and the effects of adjacent gob gas ventholes (GGVs) on NIOSH boreholes drilled in the study panel. Three different stratigraphic horizons were monitored by the NIOSH boreholes. Results indicated that the gob gas venthole fracture network formed 24 to 46 m (80 to 150 ft) ahead of the mining face. Overburden permeabilities within the same overburden test zones were ~1 md prior to undermining, increasing to hundreds or thousands of md during undermining. Permeabilities measured seven months after undermining showed additional increases. The relationship between changing reservoir conditions, longwall face position, and surface movement is discussed. Recommendations are made to optimize GGV performance by evaluating changes in subsidence produced by mining, resulting in rock stresses that substantially influence induced fracture permeability. Mechanisms to account for the observed changes in reservoir conditions are reported.

Published by Elsevier B.V.

1. Introduction

The National Institute for Occupational Safety and Health (NIOSH) is active in ventilation and methane control research to improve worker safety in underground coal mines. Methane emissions from longwall gob gas reservoirs must be effectively managed to maintain safe mine operations since they produce an estimated 80–94% of total mine emissions (Curl, 1978; Schatzel et al., 1992). The collapse, caving, and fracturing of adjacent rock units during undermining greatly influence changing reservoir conditions for coal mine gob gas. Gob gas is typically controlled in the US with stimulated vertical boreholes, in-seam boreholes, and gob gas ventholes (also known as "gas vent boreholes"). Less common in the US are cross-measure boreholes as a means of capturing gob gas.

The control of gob gas can be enhanced by reducing the methane content of the mined coal bed and the adjacent coal units. A range of in-seam boreholes is in use within the US coal mining industry for this purpose, including short (less than 150-m [500-ft]) in-seam boreholes, long directionally drilled holes collared and drilled from within mine workings, and holes directionally drilled and collared at the surface.

Although the performance of individual methane drainage boreholes can be numerically simulated, the degree of interaction between multiple holes and their cumulative effect on methane emissions underground can be difficult to establish. The complexity of the methane migration and removal scenario is exacerbated by substantial changes occurring in the reservoir due to longwall mining-induced caving and fracturing of strata near the mined coal bed. The extent of caved and fractured zones has been discussed in previous research, but can be strongly influenced by site-specific variables (Singh and Kendorski, 1981). A range of modeling methods are being used to predict methane drainage borehole interactions and changing underground emission rates (Zuber, 1998; Balusu et al., 2001; Karacan, 2007, 2008). These techniques will continue to evolve and measured field results will further develop and calibrate the simulations.

This research was designed to provide direct measurement of changing reservoir conditions during longwall mining that can enhance methane removal and control methods, thereby improving underground mine safety. To achieve these goals, NIOSH and a cooperating mine operator began a collaborative research effort to monitor reservoir parameters from gob gas ventholes (GGVs). During the experiment, other measurements were also made to determine surface movements and longwall face locations. The planned research outputs reviewed in this paper include an enhanced understanding of trends in changing gob reservoir conditions during mining, a correlation of surface deformation and face position to changes in reservoir conditions, a summary of mechanisms that produce the observed trends, and recommendations for GGV design parameters.

1.1. Background

1.1.1. Gas and air movement in gobs

Successful management of coal bed gas emissions into mine workings requires knowledge of the flow and flow paths of methane gas

* Corresponding author. Tel.: +1 4123866521; fax: +1 4123866595.
E-mail address: zia6@cdc.gov (S.J. Schatzel).

0013-7952/$ – see front matter. Published by Elsevier B.V.
doi:10.1016/j.enggeo.2012.01.002

and ventilation air in the gob. Techniques to determine these rates and movements include direct measurements of gas concentrations and flow rates and numerical modeling methods (Lunarzewski, 1998; Karacan et al., 2007). Tracer gas studies can yield similar gob gas migration information when compared to the measured concentration and flow data (Timko and Thimons, 1982; Vinson and Kissell, 1986; Young et al., 1997).

Behaviors of gob gas movement which are agreed upon by previous investigations include the following: permeability in longwall panel overburden increases after mining; after undermining, the surface above the longwall panel subsides to a lower elevation as the void space formerly occupied by the mined coal is partially in-filled by broken overburden; a zone of increased permeability exists in longwall overburden above the caved zone of a longwall panel. This increased permeability zone parallels the gateroads and resides near tailgate and headgate gateroads.

1.1.2. Subsidence theory

Longwall mining-induced fracturing associated with strata subsidence creates a distribution of high permeability pathways in gobs that greatly influence gob gas and ventilation air migration (Esterhuizen and Karacan, 2007). Investigations of surface subsidence and predictive models have predicted the depth and shape of the subsidence trough (Adamek et al., 1987). The generation of predictive mine subsidence models was the subject of multiple investigations in the Northern Appalachian Basin (NAB) (Jeran et al., 1986; Matetic and Trevits, 1990). Pre-existing formation and fracture permeability are likely overcome by the magnitude of mining-induced fracture permeability. Consequently, in all portions of the gob fractured by the mining process, gas movement is primarily dictated by ground movement of the collapsed and fractured rock associated with removal of the mined coal bed.

The prediction of surface subsidence is largely based on strata subsidence models including Bals' theory, which states that forces acting on the overburden are in response to the mined-out coal bed void spaces (Bals, 1931, 1932; Adamek et al., 1987). However, the pathway by which forces are expressed from the mined unit to the surface is not well defined by Bals' theory. The development of tensional and compressional zones during longwall mining is highly influential in defining gas migration pathways in fractured rock. When undermined, the strata near the panel margins are under tension and regions near the center of the panel development, near the long axis centerline, are under compression. In general, the fractures under tensional stress tend to be held open, increasing permeability, compared to those areas under compressive forces that tend to close rock fractures (Diamond et al., 1994). Therefore, the distribution of tensional and compressional zones in the overburden is strongly related to fracture permeability and GGV performance during panel extraction.

2. Description of the borehole monitoring experiment (BME) methodology on an active longwall panel

The field experiment consisted of three boreholes, BH-1, BH-2, and BH-3, drilled from the surface above a longwall panel into three different stratigraphic zones. The study panel dimensions were 442 m (1450 ft) in width and 3456 m (11340 ft) in length. The distance to the tailgate gateroads for each borehole was 101 m (330 ft), the same distance that the mine used for its GGVs so that they would be in the same mechanical behavior zone and in a similar stress field (Fig. 1). One of the operator's GGVs was located 76 m (250 ft) from the most outby borehole in the study, and was included in the BME monitoring activities. The spacing between each of the NIOSH monitoring boreholes was 15 m (50 ft).

The collar elevations of BH-1, BH-2, and BH-3 were 418.61 m (1373.4 ft), 414.65 m (1360.4 ft), and 410.23 m (1345.9 ft), respectively, with a coal elevation of 158 m (519 ft). The first borehole intercepted by mining (BH-1) was drilled to a total depth of 220 m (721 ft) to monitor the Sewickley Coal bed (Fig. 2). The second, or middle-range borehole (BH-2), was drilled to a depth of 230 m (755 ft) and monitored mostly shale sequences below the Sewickley Coal bed. The deepest borehole (BH-3), closest to the GGV, was drilled to 245 m (803 ft) for monitoring shale and sandstone horizons above the Pittsburgh Coal bed that would be retained in the caved zone of the gob after undermining. Boreholes were drilled with a 15-cm (6.0-in) diameter bit with water as the drilling fluid. The boreholes were cased with 13-cm (5.0-in) steel casing. They were cemented using conventional grout and cement baskets, except for the bottom 6.1 to 9.1 m (20 to 30 ft). These sections were cased with slotted casing and were the primary monitoring zones for each hole. The length of slotted casing was 9.1 m (30 ft) in BH-1 in order to monitor both splits of the Sewickley Coal bed. The slotted section of BH-2 was 6.1 m (20 ft) long. The last 2.4 m (8.0 ft) of the hole below 3.7 m (12 ft) of slotted casing of BH-3 was cut and left open-hole in order to keep the casing as high as possible above the gob (Fig. 2).

After the completion of drilling, the deepest borehole (BH-3) was logged open-hole with density, gamma ray, and sonic tools to identify formations, to refine drilling depths, and to calculate porosity, density, and some of the mechanical properties of the rock. The drilling of the boreholes was started and completed when the longwall face was 760 m (2500 ft) away from the BH-1 location.

The experimental boreholes were configured to be completed in a manner similar to the mine operator's GGVs. Both borehole designs included flame arrestors, shut-in valves, and long, vertical PVC pipe stacks. However, unlike the experimental boreholes, the GGVs were cased with 61 m (200 ft) slotted casing at the bottom of all boreholes. The NIOSH test boreholes were shut-in throughout the monitoring duration.

2.1. Instrumentation and monitoring

An important portion of this study involved measurements of in-situ permeability before and after the undermining of the NIOSH borehole sites. These tests also provided valuable data on water production from the slotted casing sections. The initial pre-undermining findings present data on the initial water saturations of the formations of interest. Boreholes were equipped with submersible, downhole transducers which were positioned within the downhole monitoring zones. Downhole transducers were installed underwater in the boreholes to record transient changes of the water head in the boreholes with a downhole data logger and an attached cable. A set of slug tests was designed and performed in each borehole using water to determine formation permeabilities. The water head drop was monitored for about a week on each borehole using the submersible transducers before the boreholes were undermined. After the conclusion of the slug tests, the downhole transducers were repositioned above slotted sections in each borehole.

The slug tests were performed by filling the boreholes with additional quantities of water so that a change in water head could be observed. This water monitoring interval was included to provide input on pre-mining permeabilities, strata disturbances, fracture initiation with respect to the position of the longwall face, and the transient fracture permeabilities induced by mining. The submersible transducers recorded changes in water head until the water drained completely from the boreholes. The final set of slug tests was run after the completion of the panel for determining post-mining permeabilities.

The wellheads on BME boreholes also were equipped with surface pressure transducers for continuous data recording of pressure changes at the tops of the boreholes. Tiltmeters were installed on the BME wellhead stacks for recording subsidence and strata-response profiles before, during, and after mining. Conventional

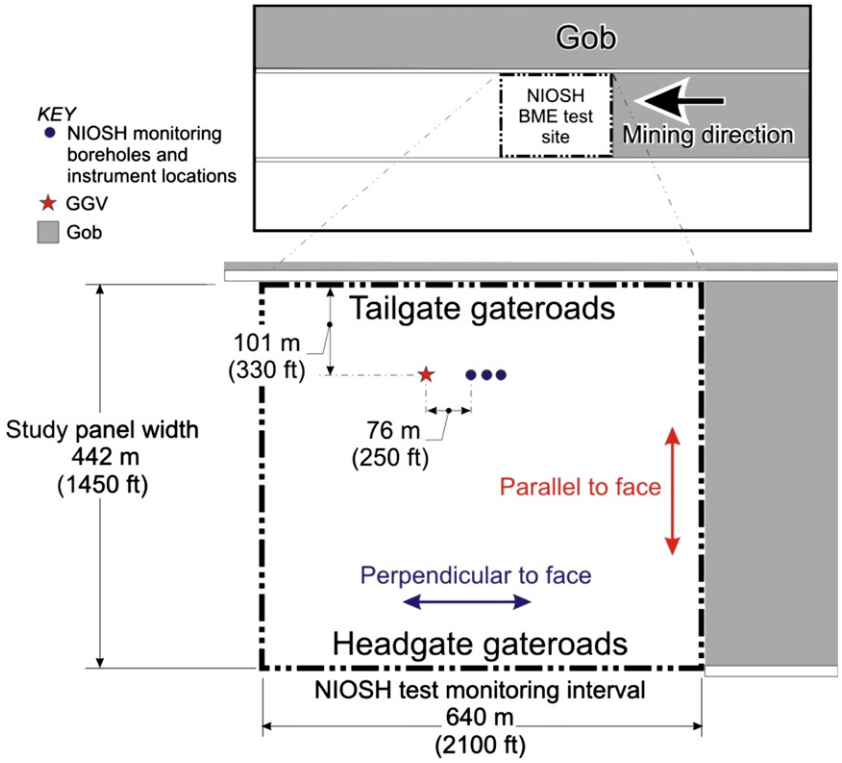

Fig. 1. The study site is shown over an active longwall panel.

positional surveys on the surface were scheduled to track the movement. The longwall face position was recorded daily. Pressure and methane concentration readings at the surface were taken regularly to monitor the changes in the wellbores as a result of the mining-induced fracturing of strata. Pressure, flow rate, and methane concentration readings were also monitored at the nearby GGV to evaluate the underground interactions with the NIOSH boreholes. Before and after the NIOSH boreholes were undermined, a distance of 305 m (1000 ft) was selected as the primary experiment test zone. This distance was chosen based on the overburden depth and typical subsidence profiles from the Northern Appalachian Basin. All instrumentation was installed and the boreholes shut-in when the longwall face was 366 m (1200 ft) away from the first borehole.

3. Discussion of results

3.1. Permeability changes occurring in overburden

In order to quantify permeability changes in the overlying strata during mining, a slug test model for confined, anisotropic aquifers of infinite or semi-infinite in radial extent was utilized (Dawson and Istok, 1991). All permeability measurements were made with data produced from slug testing. The calculated initial permeabilities determined by the slug tests for BH-1, BH-2, and BH-3 were 2.8 md (millidarcies), 0.1 md, and 0.2 md for the Sewickley Coal bed, shale and limestone, and for the Pittsburgh Coal bed shale overburden, respectively. These data were measured immediately after the borehole

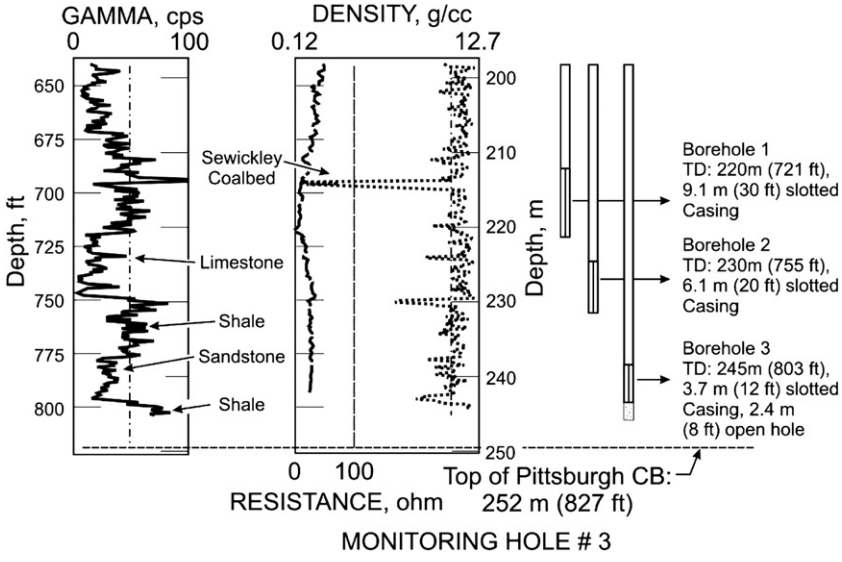

Fig. 2. Coalbed stratigraphy for the three NIOSH boreholes drilled over study panel.

stacks were assembled and prior to the formation of mining-induced fractures in the BME test zone. Following the pre-mining phase of permeability testing, downhole communication with the deepest borehole (Pittsburgh Coal bed) was lost and could not be reestablished. Thus, none of the figures include downhole pressure data from BH-3.

Fig. 3 shows the change in water head pressure in the first borehole (Sewickley Coal bed) and second borehole (shale and limestone zone between the Pittsburgh and Sewickley Coal beds). The figure shows the effect of mining disturbances on water level changes in the boreholes. The data show that the initial water head drop in the first and second boreholes occurred before the boreholes were undermined. This suggests that the initial water head decrease is associated with fracturing and/or shearing of the strata ahead of the face by about 3 days in BH–1 and about 2 days in BH–2. Fig. 3 has other implications with regard to impacts of longwall mining on reservoir properties. For instance, the water level drop confirms that there is new permeability pathways created either by the shearing or by fracturing of strata.

Water head data suggest that mining-induced disturbances forming the GGV fracture network occurred 24–46 m (80–150 ft) ahead of the mining face (Fig. 4). Water loss from the boreholes increased significantly when fractures intercepted the borehole annulus. The rate of water loss was rapid up to about 30 m (100 ft) above the mined coal bed which limited the duration of monitoring to three or four days, when the loss of water was complete. The variable rate of water loss was not related to the depth of the borehole but changed as the strata responded to fluctuations in rock stress resulting in a range of permeabilities. Damage to the borehole is likely produced by shearing and deformation in the overburden and is typically severe in near-margin GGVs where shear forces can modify the borehole annulus.

Fig. 4 shows water head and zones of averaged, instantaneous permeability as the mine face approached BH-1. The data show that as soon as the strata are affected from mining disturbances, there is an initial permeability increase. The averaged value of this initial permeability increase was ~300–400 md. After this initial increase, permeability decreased to 100 md. This permeability change behavior indicates that the initial reservoir disturbance is due to shearing and fracturing of the strata or bedding planes. After the borehole was undermined, averaged permeability increased to ~400 md due to larger-scale fractures. The highest instantaneous permeabilities measured in the borehole occurred just after disturbances first affected the coal bed (over 800 md), during the start of significant ground

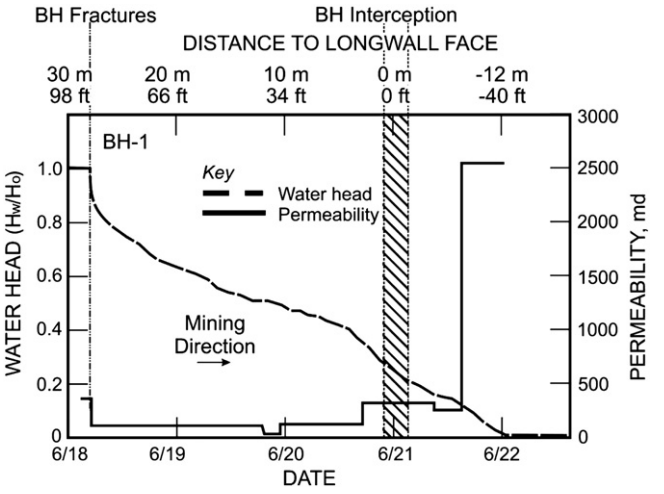

Fig. 4. Decreasing water head and changing permeabilities are shown for BH-1 during undermining. Substantial permeability changes occurred during the slug test with short duration peaks in the hundreds to thousands of md.

movement and during the undermining of the borehole location. Water loss from BH-1 began with the initial fractures which intercepted the borehole and then lost water at a relatively stable rate until the face neared the borehole and the rate of water loss accelerated. The highest averaged fracture permeability for any of the segments in the Sewickley horizon occurred after the face had passed the BH-1 location as the last of the water left the borehole (Fig. 4).

Borehole 2, designed to monitor a 6.1-m (20-ft) section in the shale and limestone zone between the Sewickley and Pittsburgh Coal beds, is analyzed using the same approach. The data in Fig. 5 show that permeabilities in BH-2 gradually increased to the 100–200 md range, possibly due to bedding plane movements. Fig. 5 shows that a sudden drop in water head occurred with an associated permeability increase at BH-2 just before undermining, where the segment averaged about 300 md. This increase coincides with the approach of the longwall face and may suggest communication between these two wells. Shortly after undermining, large-scale horizontal and vertical fractures are created and the permeability increases to about ~1600 md. Permeabilities measured prior to undermining were in the ~1 md range. Formation and fracture permeabilities gradually increase as mining-induced disturbances progress to the borehole locations. However, the biggest average change occurs following the

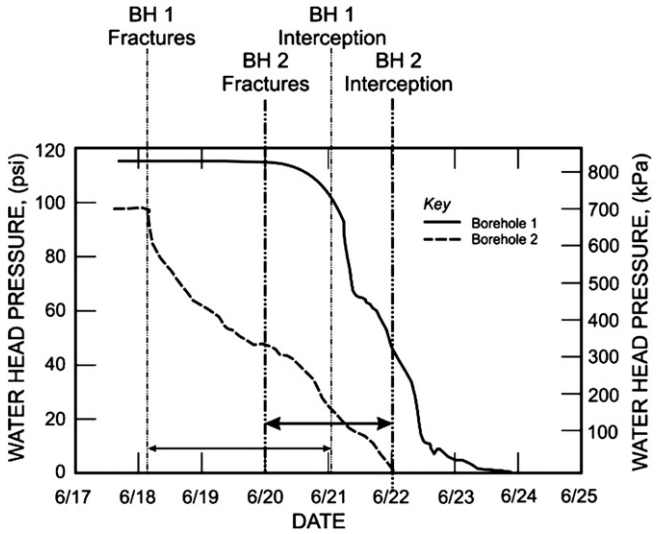

Fig. 3. Changes in water head pressure over time at boreholes BH-1 and BH-2.

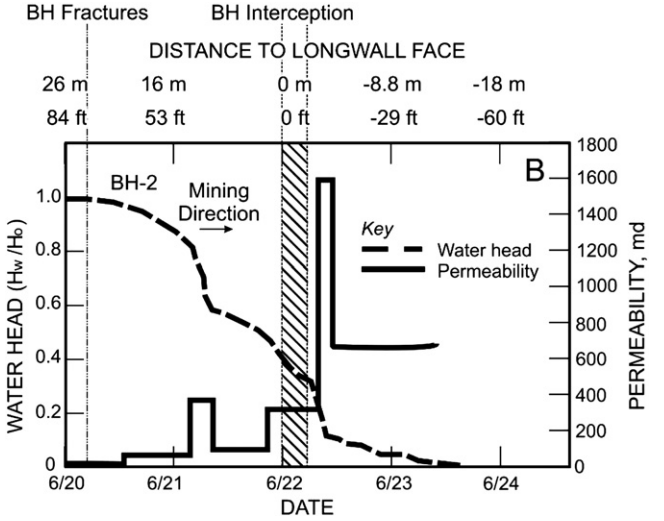

Fig. 5. Changing water head and permabilities are shown for borehole BH-2 during undermining.

interception of borehole locations. Although the test method allows for the determination of changing permeabilities as mining progresses, a disadvantage is the lack of data once all water is lost from the borehole.

As longwall mining neared completion of the study panel, the final slug tests were performed on both BH-1 and BH-2. When adding known amounts of water to the boreholes, the rate of water head loss was rapid and the interval above the transducers was emptied in a matter of minutes. In both holes, a second slug of water was added to retest borehole permeability. Borehole 1 measured 63 and 65 darcies in two tests. Consequently, BH-1 underwent a substantial increase in permeability compared to the prior maximum measured immediately following undermining (Fig. 4). When performing the slug test in BH-2, no water head build-up was achieved due to water leaving the borehole at such a rapid rate that a permeability value could not be determined. The final permeability level for BH-2 was apparently far above what was measured in BH-1. The higher permeability in the BH-2 is most likely associated with increased fracture apertures at the lower stratigraphic horizon (shale and limestone interval) when compared to BH-1 (Sewickley Coal bed); BH-2 it is closer to the void space in the caved zone. Since this relationship is reported by many mine operators, it is probable that the permeability increase close to the mined coal seam compared to positions at higher elevations is the product of spatial controls and stress regimes and not lithologic parameters.

3.2. Permeability distributions and surface movement

3.2.1. Subsidence

To optimize GGV performance, past research by the US Bureau of Mines and its successor, the NIOSH Office of Mine Safety and Health Research, showed that significant gas production improvements could be made by choosing borehole sites in zones of overburden rock tension (Diamond et al., 1992, 1994). It was recognized that enhanced GGV performance can be achieved by utilizing the high permeability zone associated with mining-induced fractures where fractures under tension yielded the highest permeability. Consequently, locations where optimal GGV performance will be achieved can be chosen on the basis of high permeability zones produced after mining. Although analyses of post-longwall mining permeability distributions have been provided for the Northern Appalachian Basin, the resolution of this distribution is not yet sufficient to allow for the selection of the optimal GGV locations (Esterhuizen and Karacan, 2007).

As a proxy for permeability distributions, recommendations for enhanced GGV performance are made for the cooperating mine on the basis of the surface deformation above the longwall study panel. The objective of this evaluation was to identify stress zones where the overburden fracture network is in tension and increased fracture permeability exists. Subsidence models for the Northern Appalachian Basin (NAB) have been shown to reliably predict surface deformation above longwall panels (Jeran et al., 1986; Adamek et al., 1987). However, when this work was performed, typical longwall panels were subcritical from an engineering perspective (the panel width was less than the depth of panel overburden). Most current NAB panels are much wider than those previously modeled, with panel width exceeding the overburden depth (supercritical panel design).

Measurements of surface movement include continuous tilt meter data and periodic conventional ground surveys. The series of conventional positional surveys performed as part of this study depicts the deformation of the surface at the NIOSH borehole sites. No surface movement was measured at any of the boreholes before the longwall face undermined the beginning of the primary test zone, which was 305 m (1000 ft) ahead of the first NIOSH borehole. Measurable vertical movement of 0.003 m (0.01 ft) occurred at one borehole collar when the face was positioned 20 to 51 m (66 to 166 ft) from the three NIOSH boreholes.

To analyze surface deformation at the study site, predictive model simulation is preferred to field data since models are not influenced by site-specific features. Methods have been published for predicting surface deformation and the resulting curve for the study site is shown in Fig. 6. One predictive method utilizes a theoretical evaluation of surface deformation (Bals, 1931, 1932). Subsidence data are plotted relative to face data (x axis 1) and model data are plotted relative to the panel edge (x axis 2). Consequently, the plot includes data for dynamic and static subsidence curves (field data and model data, respectively).

The field data subsidence curve includes combined data relative to face position from all three boreholes. The field data and the predictive subsidence curve plot have different y intercepts (Fig. 6). The subcritical design of the longwalls included in the development of the predictive subsidence curves is thought to be largely responsible for the apparent offset between theses graphs and the supercritical field data. For application to the field site, the model data were adjusted to move the model curve towards the center of the panel to match the field data y intercept. This 17-m (55-ft) offset for the modified "a" value curve is used in subsequent analysis of surface movement (Fig. 6).

Fig. 7 shows a plot of permeability changes measured at boreholes BH-1 and BH-2 during undermining as a function of subsidence. The subsidence data set used in the plot was the model data from the modified calculated "a" curve shown in the previous figure. Both permeability and subsidence increases were measureable as mining approached the boreholes. During the undermining of the NIOSH boreholes, measured permeabilities were on the order of 300 md. Increases in permeability relative to subsidence occurred sooner in BH-2 than in BH-1, which is expected to be a function of the lower stratigraphic position of monitored horizon in BH-2. The lower stratigraphic position of the BH-2 monitored zone is places it closer to the caved zone in the gob and probably means the developing fractures have a greater aperture than when they reach BH-1. However, Fig. 7 shows that the highest averaged permeabilities were higher in BH-1 than BH-2. This maximum value may be a function of water retention in the borehole and BH-2 may have lost its water too soon to produce a higher permeability value due to its closer proximity to mine workings. The increase in permeabilities measured in both boreholes corresponds to the longwall face position having passed beneath the boreholes and the period when GGVs typically reach their maximum production potential. Other permeability analyses have been conducted in similar stratigraphy which also addressed GGV production and related factors (Karacan, 2009; Karacan and Goodman, 2009).

An additional plot is shown to select the recommended borehole location from the subsidence data (Fig. 8). Curvature is proportional to strain and therefore shows where the overburden fractures are expanded or contracted. The y axis units for the curvature plots are shown as inverse distance where the positive values are proportional to tension and the negative values are proportional to compression. The high tension zones shown by the plots depict areas where fracture permeability is high and advantageous for gas transport to methane drainage boreholes, with inflection points indicating changing rock stress conditions. The ground instability associated with these areas of changing rock stress makes these locations undesirable for GGV sites. No lateral or horizontal movement indicative of lateral stress was recorded at any of the NIOSH boreholes.

3.2.2. Surface tilt

Surface tilt data recorded during the study provide continuous data relating to surface movement and mining-related permeability development in longwall overburden. Surface tilt measured at the three NIOSH boreholes is shown in Fig. 9. One conventional measure

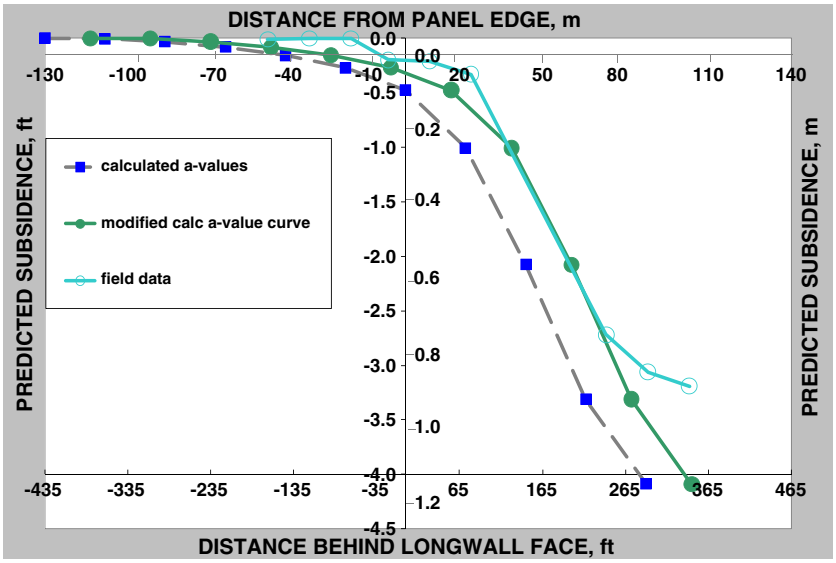

Fig. 6. Subsidence curves are shown for the study panel where negative distance is measured from the panel margin outward. Axis x1 shows distance from panel edge; axis x2 shows distance behind face.

of surface tilt depicts data in mm/m, as is shown in the figure. Tilt data are shown plotted relative to longwall face position for the three NIOSH boreholes. The figure shows the averaged data set from all three NIOSH boreholes recorded for tilt both parallel to the mine face (x) and parallel to the mining direction (y). Also shown on the plot are the subsidence data from modeling of the subsidence in the NAB and modified using field data from this study (Jeran et al., 1986; Adamek et al., 1987).

Tilt parallel to the longwall face did not return to the pre-mining position, but tilt parallel to the face did return to nearly the pre-mining orientation (Fig. 9). Surface tilting in the mining direction was measurable when the longwall face was 91 m (300 ft) from the boreholes, prior to undermining. Tilt reached maximum in this direction when the face was about 61 m (200 ft) past the boreholes or about 1 month after undermining. This location corresponds to about the midpoint or inflection point on the tilt curve parallel to the face.

Fig. 10 shows the average change in tilt occurring at the three NIOSH boreholes relative to longwall face position. Maximum tilt in the direction of mining occurs about 15 m (50 ft) behind the face. The majority of surface movement or tilting ceases in this y direction after the face is about 190 m (620 ft) past the monitoring site with all movement ceasing after the face has reached a position about 210 m (700 ft) past the site. Tilt measured parallel to the mine face in the x direction reached a maximum at 27 to 40 m (90 to 130 ft) towards the centerline from the panel margin and ceased 130 m (440 ft) from the panel margin. The maximum curvature value from the modified static subsidence model is 34 to 40 m (110 to 130 ft) (Fig. 8).

From the plot of surface curvature, the majority of vertical movement is shown to end 88 m (290 ft) behind the face in the direction of mining. Palchik (2003) reported surface movement continuing for up to 120 m (400 ft) behind a longwall face. The study site design parameters (longwall panel width, overburden depth) suggest a location for the GGVs at a near-margin position of between about 76 to 91 m (250 to 300 ft) from the panel edge (Schatzel et al., 2008). This location would place the borehole away from the site of maximum surface tilt observed in the direction of mining, 61 m (200 ft)

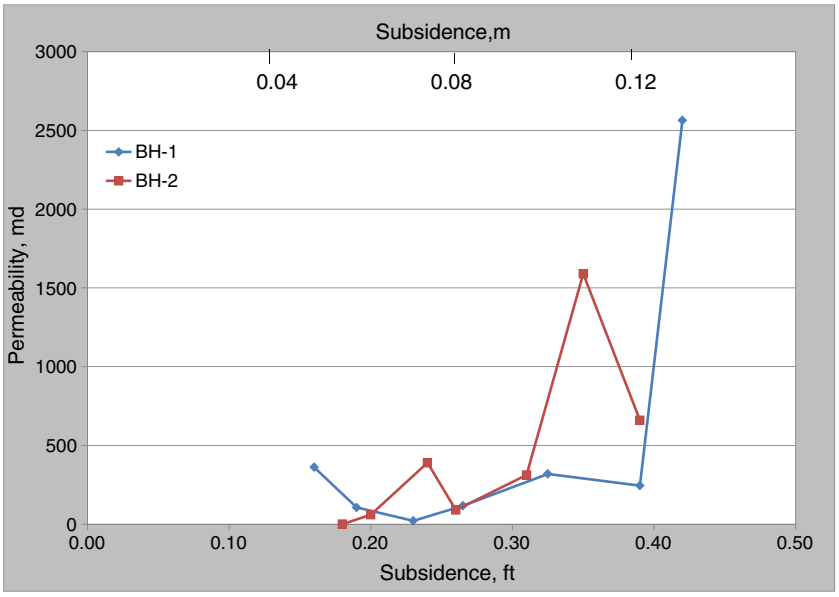

Fig. 7. Plot of averaged permeability changes at boreholes BH-1 and BH-2 relative to subsidence. Subsidence data shown are the modified a calculated values.

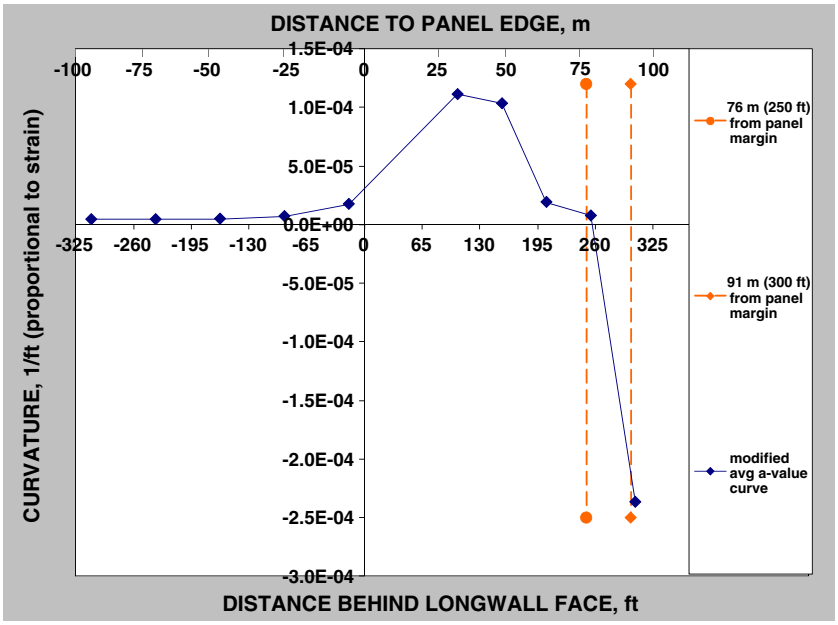

Fig. 8. Surface curvature plots are shown for the predicted subsidence curves following the 17-m (55-ft) adjustment made using field measurements from the supercritical study panel. Axis x1 shows distance from panel edge, axis x2 shows distance behind face.

past the boreholes — the same distance from the panel edge where the maximum change in tilt occurred. The location from 76 to 91 m (250 to 300 ft) inside the panel edge also includes the position where most vertical surface movement had ceased — 88 m (290 ft). The recommended position also locates the borehole outside, towards the panel margin, relative to the area of maximum compression in the central region of the panel (Fig. 8).

3.3. Field evidence of GGV performance in response to a retreating longwall face and changes in fracture permeability

Field monitoring produced data indicating how temporal and spatial permeability variations in the gob affect GGV performance. In Fig. 11 are three related graphs displaying methane concentrations in the boreholes (A), gas pressures in the boreholes (B), the location of the mine face, and (C) GGVs and other important sites on the longwall panel. As the longwall face retreated within the primary test zone towards the NIOSH boreholes, the GGV1 exhauster was operational as shown by the diagonal shading. All exhausters are methane-driven and therefore only run when a reliable, high-concentration, production gas stream is available. Methane concentrations rose to nearly 100% as the boreholes were approached and then methane concentrations and pressures dropped due to the loss of water within the casing. A work stoppage occurred with the longwall face situated under the three boreholes, two having been undermined with one hole just inby the face. Borehole GGV1 also went offline during this period of work stoppage. Data from the slug tests show that permeabilities in monitored horizons in BH-1 and BH-2 were between 650 to 2500 md while the face was at this location, although no GGV production occurred while the face was idle.

After longwall mining resumed, the undermined boreholes underwent additional fracturing (i.e., the Sewickley Coal bed horizon, the BH-1 monitoring and production zone). The releasing of methane gas increased methane concentrations and borehole pressures, and

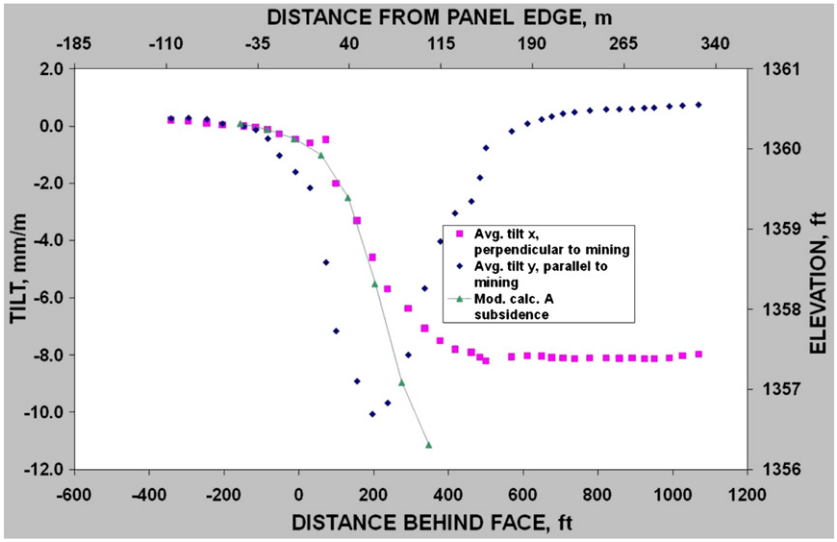

Fig. 9. The average surface tilt measured at the three NIOSH boreholes is shown as the "modified calculated A subsidence curve." The direction of mining is shown as the x direction (axis x2) and parallel to the longwall face is the y direction (axis x1).

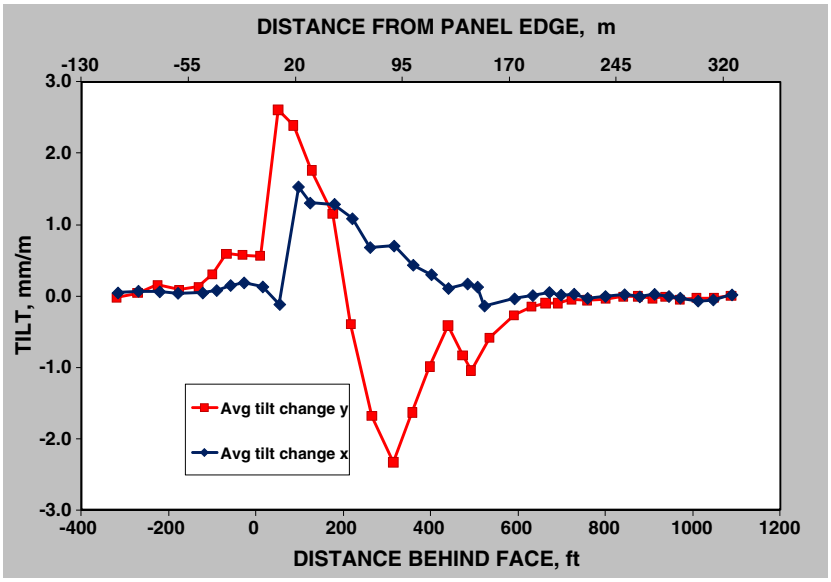

Fig. 10. Changing magnitudes of tilt measured at the NIOSH boreholes and shown as averaged curves for the x and y direction. The direction of mining is shown as the x direction (axis x2) and parallel to the longwall face is the y direction (axis x1).

GGV1 began producing gob gas via the methane-powered exhauster again (Fig. 11). In NIOSH borehole BH-3, low gas concentrations and pressure changes were observed as a result of borehole fracturing.

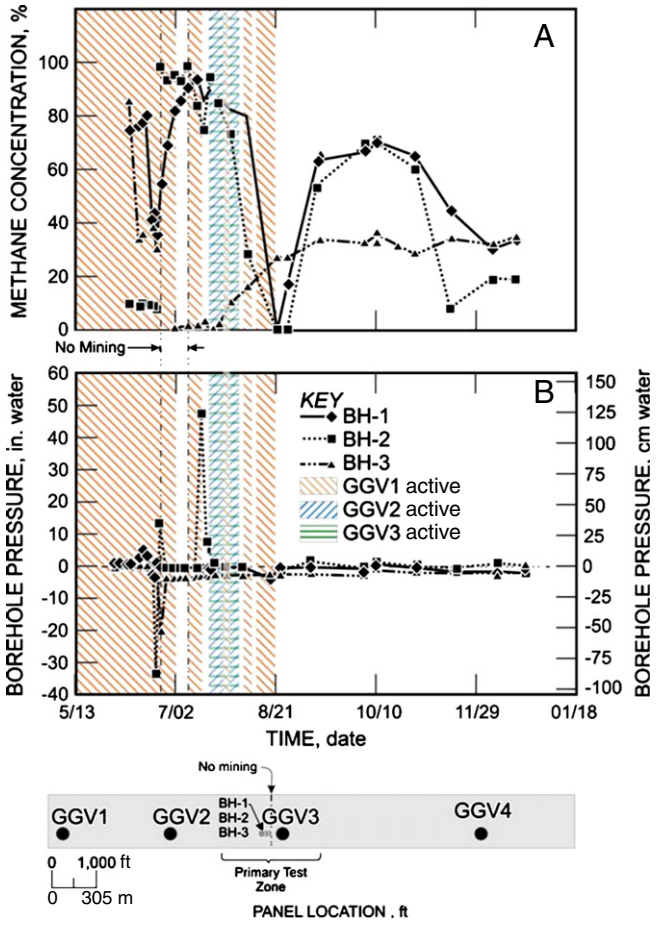

Fig. 11. Three related graphs displaying methane concentrations in the boreholes (A), gas pressures in the boreholes (B), and the location of the mine face, GGVs, and other important sites on the longwall panel. The shaded areas indicate that a GGV is operating.

This gas behavior is a product of the completion depth 7.3 m (24 ft) above the Pittsburgh Coal bed, which allowed for communication with the mine ventilation network. With continued gas production from GGV1, gas concentrations began to drop at the NIOSH boreholes and in the fractured reservoir until GGV1 ceased production. Production from GGV1 during this period lowered gas concentrations in BH-1 and BH-2 and, therefore, was in communication with these monitored intervals.

Following the resumption of mining, borehole BH-2 showed an increase in gas pressure and concentration followed by a drop in both, presumably due to fracturing and the subsequent loss of water from GGV3. Interestingly, there was an increase in gas pressure at BH-2 but not a similar gas pressure response at the Sewickley Coal bed horizon (BH-1). The initial fracture development may have not reached the Sewickley, although other data show that it will in time reach that horizon (Fig. 4). Also, the quantity of liberated gas from the initial fracture may have been small, possibly from the shale horizons associated with the BH-2 horizon, and thus the gas did not reach or pressurize the Sewickley Coal bed. Although permeability data are not available from BH-1 and BH-2 with the face retreated to this position due to the loss of water from the boreholes, it is expected that permeability did not decrease from the last levels shown in Figs. 4 and 5, about 650 and 2500 md.

As mining progressed after the work stoppage, all three GGVs produced gob gas at various time intervals although only GGV 2 and 3 produced at the same time. Gob gas production from operating GGVs decreased methane concentrations at BH-1 and BH-2 but not at BH-3 where prevailing gob conditions were observed (Fig. 11). Borehole BH-3 showed gas pressure to be close to atmospheric, consistent with mine ventilation conditions. Monitoring of the GGVs ended after the face exited the primary test zone, but continued at the three NIOSH boreholes. After the longwall face moved past GGV4, a significant drop in methane concentration was observed at BH-1 and BH-2.

In addition to the observed temporal and special changes in the fractured overburden reservoir, the study results also relate the measured reservoir parameters to borehole production. Methane concentrations and gas pressures were measured at BH-1 and BH-2 in the Pittsburgh Coal bed overburden in response to production changes occurring at all four GGVs located in the studied panel. The methane concentration changes measured during the undermining GGV-1

and 4 indicate that the gob was highly communicative with responses observed at distances on the order of 1500 m (5000 ft) from the monitoring location. A series of prior NIOSH tracer gas research studies produced similar findings (Mucho et al., 2000). At these distances, gob permeability in BH-1 and BH-2 is at a maximum of 63–65 darcies (Sewickley Coal bed horizon) and over 65 darcies (shale and limestone interval between the Sewickley and Pittsburgh Coal beds), respectively. At these positions behind the face, maximum subsidence will have occurred near the longwall panel centerline (Fig. 12). These data indicate that maximum subsidence along the centerline corresponds to maximum permeability in the longwall panel overburden in the vicinity of the near-margin GGVs.

3.4. Mechanisms responsible for observed changes in gob permeability

Data from this study show that improved GGV performance was directly related to surface deformation and increased subsidence. The increased permeability over the gateroads during maximum overburden compaction has not been previously reported. An enhanced understanding of this relationship may provide additional input to mine operators in optimizing GGV site selection for improved gob gas production and better adherence to underground, statutory methane concentrations.

Two mechanisms are recognized as potentially contributing to the increase in fracture permeability during overburden compaction. The first is the draping effect in the tensional zone of the overburden. The overburden connecting the compacted zone over the longwall panel to the largely un-compacted zone over the gateroads is in tension, and this overburden achieves maximum fracture permeability during maximum compaction of the gob (Fig. 13). A second mechanism which may contribute to the onset of the final fracture permeability levels in the overburden is coal matrix shrinkage. A loss of coal volume within the matrix occurs when coal bed gas migrates out of the coal matrix in response to the decrease in gas pressure within the coal fracture system. In this scenario, there is swelling of the coal matrix due to coal bed gas retention and shrinkage of the matrix during the loss of that gas.

For this study, the two mechanisms are likely producing a combined effect in the permeability increase measured in the near-margin GGV monitoring intervals. It is assumed that no additional changes occurred in permeability after the last period of subsidence monitoring (three months after undermining) and prior to the period of final permeability slug tests (seven months after undermining).

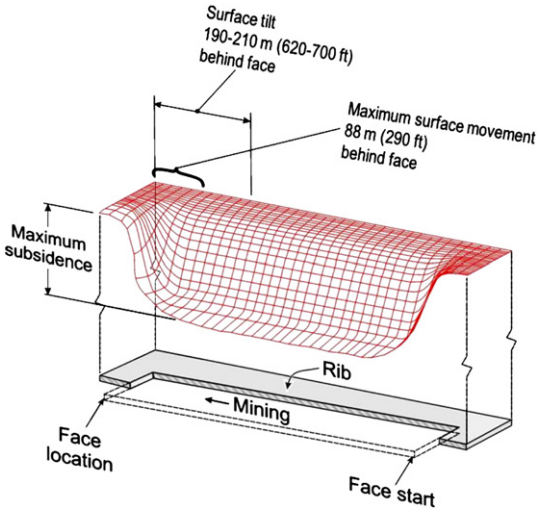

Fig. 12. Diagram of the surface subsidence trough over an active longwall panel (not to scale). Results from this study show that vertical surface movement is complete at about 88 m (290 ft) behind the longwall face.

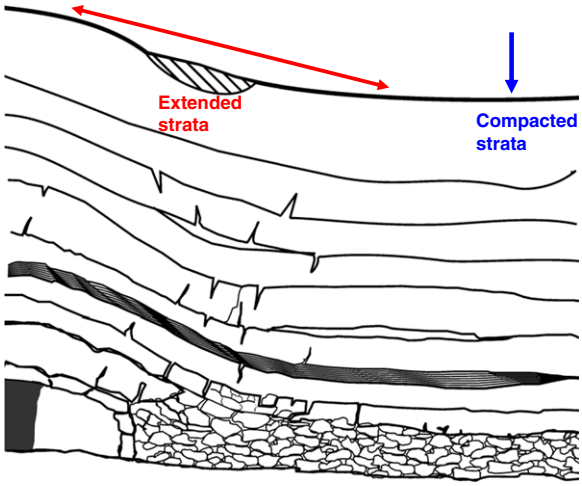

Fig. 13. A hypothetical cross-section (not to scale) of a longwall panel gob viewed parallel to the face and extending from the panel margin to the panel centerline.

This assumption is consistent with subsidence theory, where natural forces provide the only impetus for the progression of surface movement as long as the rate of overburden compaction allows for maximum subsidence in the three-month time frame, during which mining progressed about 838 m (2750 ft) from BH-2 located at the center of the NIOSH test monitoring interval.

4. Summary and conclusions

This research provided direct measurement of changing reservoir conditions during mining in longwall panel overburden that would influence methane removal and control methods. In this study, a borehole monitoring experiment (BME) was designed to measure changes in reservoir parameters and associated variables affecting gas transport via methane drainage boreholes. The loss of water from GGVs, indicating fracturing in the strata, was rapid at distances of 30 to 22 m (100 ft to 72 ft) above the mined coal bed. The rate of water loss was not related to borehole depth. Overburden permeabilities within the same overburden test zones ranged from ~1 md range prior to undermining. Averaged permeabilities increased 100 to 500 times following undermining with higher instantaneous peaks observed. This increase in permeability occurred after the longwall face undermined the monitored locations.

Permeability changes in longwall panel overburden are produced by rock stresses and induced fractures in these strata. Tensional and compressional rock stresses are produced as the overburden extends into underground void space formerly occupied by the mined coal bed. An analysis of surface subsidence identified these stress regimes. The analysis of surface movement was used as a proxy for the distribution of fracture permeability in the longwall gob overburden. The recommended site for the GGVs was chosen to be between zones of maximum surface movement and zones of maximum compression. Evidence of surface tilting in the direction of mining began about 91 m (300 ft) before the boreholes were undermined, reaching a maximum at 61 m (200 ft) behind the face. The majority of surface subsidence was observed to end about 88 m (290 ft) behind the face. Recommendations to the mine operator for the study panel configuration (442 m face length, 270 m of cover [1450 ft face length, 900 ft of cover]) were to place GGVs between 76 and 91 m (250 to 300 ft) from the tailgate panel margin.

With GGVs located about 101 m (330 ft) from the tailgate margin, gob gas venthole production affects gas pressure and methane concentration in the fractured gob overburden at distances of at least 1500 m (5000 ft) along the longwall tailgate panel margin. At closer borehole spacings, production from a particular borehole is

influenced by adjacent borehole activity. Two mechanisms are recognized as potentially contributing to the increase in fracture permeability during overburden compaction. The first is the draping effect in the tensional zone of the overburden. The second is coal matrix shrinkage due to a decrease coal bed gas pressure. Since the highest overburden permeabilities are achieved months after undermining, once maximum compression is realized, gob gas removal via GGVs can best take advantage of this post-undermining period by placing the borehole in a stable site.

Disclaimer

The findings and conclusions in this report are those of the authors and do not necessarily represent the views of the National Institute for Occupational Safety and Health.

References

Adamek, V., Jeran, P.W., Trevits, M.A., 1987. Prediction of surface deformations over longwall panels in the northern Appalachian Coalfield. US Bureau of Mines RI9142.

Bals, R., 1931, 1932. Beitrag zur Frage der Vorausberechnung Bergbaulicher Senkugen (A contribution to the Problem of Precalculating Mine Subsidence). Mitteilungen aus dem Markscheidewesen 42/43, 98–111 (in German).

Balusu, R., Deguchi, G., Holland, R., Moreby, R., Xue, S., Wendt, M., Mallet, C., 2001. Goaf gas flow mechanics and development of gas and Sponcom control strategies at a highly gassy coal mine. Papers and presentations from the Australia–Japan Technology Exchange Workshop, Dec. 2–4, Hunter Valley.

Curl, S.J., 1978. Methane Prediction in Coal Mines. IEA Coal Resources Report ICTIS/TR 04.

Dawson, K.J., Istok, J.D., 1991. Aquifer Testing: Design and Analysis of Pumping and Slug Tests. Lewis Publishers, Inc., Chelsea, Michigan.

Diamond, W.P., Ulery, J.P., Kravits, S.J., 1992. Determining the Source of Longwall Gob Gas: Lower Kittanning Coalbed, Cambria County, PA. U.S. Department of the Interior, Bureau of Mines. Report of Investigations 9430, NTIS No. PB 93-132058, pp. 1–15.

Diamond, W.P., Jeran, P.W., Trevits, M.A., 1994. Evaluation of Alternative Placement of Longwall Gob Gas Ventholes for Optimum Performance. U.S. Department of the Interior, Bureau of Mines. Report of Investigations 9500, NTIS No. PB 94-171949, pp. 1–14.

Esterhuizen, G., Karacan, C.Ö., 2007. A methodology for determining gob permeability distributions and its application to reservoir modeling of coal mine longwalls. Proceedings, Annual Mtg., Society for Mining, Metallurgy, and Exploration, Denver, CO.

Jeran, P.W., Adamek, V., Trevits, M.A., 1986. A subsidence prediction model for longwall mine design. SME-AIME Fall Meeting, St. Louis, MO. September 7-10, pp. 3–8.

Karacan, C.Ö., 2007. Evaluation of the relative importance of coalbed reservoir parameters for prediction of methane inflow rates during mining of longwall development entries. Computers & Geosciences 34 (9), 1093–1114.

Karacan, C.Ö., 2008. Modeling and prediction of ventilation methane emissions of US longwall mines using supervised artificial neural networks. International Journal of Coal Geology 73, 371–387.

Karacan, C.Ö., 2009. Reservoir rock properties of coal measure strata of Lower Monongahela Group, Greene County (Southwestern Pennsylvania), from methane control and production perspectives. International Journal of Coal Geology 78, 47–64.

Karacan, C.Ö., Goodman, G., 2009. Hydraulic conductivity and influencing factors in longwall overburden determined by using slug tests in gob gas ventholes. International Journal of Rock Mechanics and Mining Sciences 46 (7), 1162–1174.

Karacan, C.Ö., Esterhuizen, G.S., Schatzel, S.J., Diamond, W.P., 2007. Reservoir simulation-based modeling for characterizing longwall methane emissions and gob gas venthole production. International Journal of Coal Geology 71, 225–245.

Lunarzewski, L.W., 1998. Gas emission prediction and recovery in underground coal mines. International Journal of Coal Geology 35, 117–145.

Matetic, R.J., Trevits, M.A., 1990. Case study of longwall mining effects on water wells. Society of Mining Engineers Annual Meeting, Feb. 26–Mar. 1, Salt Lake City, UT.

Mucho, T.P., Diamond, W.P., Garcia, F., Byars, J.D., Cario, S.L., 2000. Implications of recent NIOSH tracer gas studies on bleeder and gob gas ventilation design. Society of Mining Engineers Annual Meeting, Feb. 28-Mar. 1, Salt Lake City, UT.

Palchik, V., 2003. Formation of fractured zones in overburden due to longwall mining. Environmental Geology 44, 28–38.

Schatzel, S.J., Garcia, F., McCall, F.E., 1992. Methane sources and emissions on two longwall panels of a Virginia coal mine. Proceedings, 9th Annual Intl. Pittsburgh Coal Conf., Pittsburgh, PA, Oct. 12-16, pp. 991–998.

Schatzel, S.J., Karacan, C.Ö., Goodman, G.V.R., Mainiero, R.J., Garcia, F., 2008. The borehole monitoring experiment: field measurements of reservoir conditions and responses in longwall panel overburden during active mining. 12th US Mine Ventilation Symposium, Reno, NV, June 9-12, 2008.

Singh, M.M., Kendorski, F.S., 1981. Strata disturbance prediction for mining beneath surface water and waste impoundments. 1st Conf. Ground Control in Mining, Morgantown, WV, pp. 76–89.

Timko, R.J., Thimons, E.D., 1982. Sulfur hexafluoride as a mine ventilation research tool — recent field applications. U.S. Department of the Interior, Bureau of Mines. Report of Investigations 8735, NTIS No. PB83-171819, pp. 1–15. 1982.

Vinson, R.P., Kissell, F.N., 1986. Three coal mine ventilation studies using sulfur hexafluoride tracer gas. U.S. Department of the Interior, Bureau of Mines. Report of Investigations 8142, NTIS No. PB-255300, pp. 1–19. 1986.

Young, D.A., Bonnell, G.W., Genter, D.G., 1997. Tracer gas techniques for mapping air and methane migration through a longwall waste in an underground coal mine using tube bundle systems. SME Annual meeting, Feb. 26-28, Denver, CO.

Zuber, M.D., 1998. Production characteristics and reservoir analysis of coalbed methane reservoirs. International Journal of Coal Geology 38, 27–45.